stellarator news

Published by Fusion Energy Division, Oak Ridge National Laboratory
Building 9201-2 P.O. Box 2009 Oak Ridge, TN 37831-8071, USA
Editor: James A. Rome Issue 35 September 1994
E-Mail: jar@ornl.gov Phone: (615) 574-1306

Transient transport studies in W7-AS

One tool for deriving the functional dependences of the electron heat diffusivity is the comparison of the incremental diffusivity, $\chi_e^{inc} = \partial q_e / \partial(n_e \nabla T_e)$, obtained in perturbative studies with the diffusivity derived in stationary power balance analyses, $\chi_e^{pb} = q_e/(n_e \nabla T_e)$. Modulation experiments in W7-AS feature the introduction of a small temperature perturbation of typically 5%, whose propagation is diagnosed by means of a multichannel electron cyclotron emission (ECE) diagnostic with time resolution of better than 0.1 ms. Most of the experiments are conducted at densities below about 4×10^{19} m^{-3}, where the ions are sufficiently well decoupled from the electrons and radiation losses are small in the plasma region of interest so that damping of the heat wave through these loss channels is negligible. In this way, the electron heat diffusivity is determined rather than an effective value averaged over the ion and electron diffusivities. In perturbative experiments, the incremental heat diffusivity is determined from the modulated flux driven by the modulated gradient in contrast to the ratio of the flux and driving gradient, in a stationary power balance analysis. If χ_e is assumed to be ∇T_e-dependent in the form $\chi_e^{pb} \sim (\nabla T_e)^{\alpha}$, the incremental diffusivity will be enhanced by $(1 + \alpha)$, namely $\chi_e^{incr} = (1+\alpha)\chi_e^{pb}$.

At W7-AS [1] and WVII-A as well [2], no systematic difference between the stationary and perturbative values has been observed, which implies that no explicit ∇T_e-dependence exists.

Figure 1 compares χ_e^{incr} versus χ_e^{pb} in the range $0.5 < \chi_e < 3$ m^2/s. With allowance for error margins, the data are consistent with $\alpha < 0.5$. Varying the plasma parameters, density, power, and rotational transform yields the same scaling of χ_e^{incr} as for χ_e^{pb}: it decreases with increasing density, decreases with increasing rotational transform, and increases with heating power as expected from the scaling of the power balance derived values.

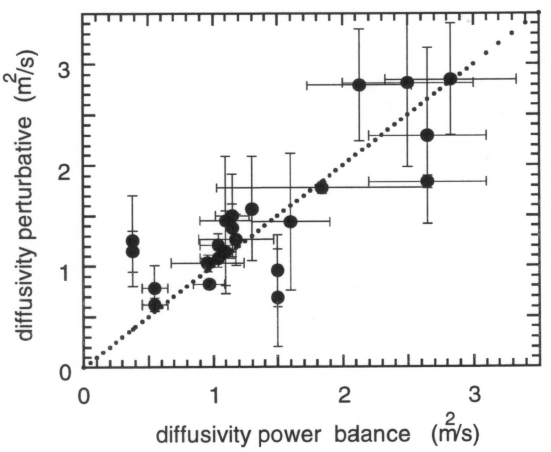

Fig. 1. The incremental electron heat diffusivity from perturbation experiments versus the diffusivity from stationary power balance analyses. No systematic difference is found, which means that no explicit ∇T_e dependence of the diffusivity exists.

In this issue . . .

Transient transport studies in W7-AS
In ECRH power modulation experiments conducted at W7-AS, neither a ∇T_e nor a T_e-dependence of the electron heat diffusivity could be derived. To explain the power degradation, a model is proposed in which the diffusivity reacts almost instantaneously to changes in heating power. 1

High current negative ion beam obtained for NBI at NIFS
The world's largest negative hydrogen ion current of 16 A was recorded at NIFS in the engineering model ion sources for neutral beam injector to be used for LHD. 3

The ATF finale
Long pulses (up to 1 h 17 min) enabled ATF to demonstrate effective wall conditioning and to perform dimensionless parameter scaling experiments. 5

Attempts have been made to derive a temperature dependence of χ_e^{pb} from the heat wave experiments. A power law dependence like $\chi_e^{pb} \sim (T_e^{\gamma})$ has two consequences. χ_e^{incr} is higher than χ_e^{pb} and, in addition, shows a modulation frequency dependence:

$$\chi_e^{incr} = [1 + c(\gamma)/f_m^{1/2}]\, \chi_e^{pb}$$

where $c(\gamma)$ is a parameter depending on the exponent γ, and f_m is the power modulation frequency. As a third indication, the temperature-dependent diffusivity introduces a nonlinearity due to a $(\nabla T_e)^2$ term entering the diffusion equation. This quadratic term is expected to generate mixing effects if more than one modulation frequency is involved simultaneously in the power modulation. In the case of two frequencies, sum and difference frequencies should appear in the Fourier spectrum of the electron temperature modulation, which are also not observed. The agreement between χ_e^{incr} and χ_e^{pb}, the missing modulation frequency dependence of χ_e^{incr}, and the lack of combination frequencies indicate that no significant T_e-dependence is present. But a power degradation is observed in W7-AS as in other devices.

As a first attempt to describe the power degradation, a model is proposed in which χ_e reacts faster than the diffusive time scale to changes in heating power [3]. The idea is based on observations made in transient transport experiments where a large amount of heating power is switched on or off, and the transient behavior of the electron temperature profile evolution is studied. The experiments were performed in purely ECRH-heated discharges (70 GHz, X2-mode) at low density, 1.5×10^{19} m^{-3}, at 1.25 T. The heating power ranged from 0.2 to 0.6 MW. Profile development is being measured by ECE. The profiles are checked against Thomson scattering profiles, with satisfactory agreement obtained. The density profiles do not change in the time intervals used for the analysis.

Power balance calculations are carried out at time slices using an analysis code, and simulations with a predictive code are performed and compared with the experimental T_e-profile evolution. The data are analyzed on the basis of a purely diffusive transport model. The analysis is started 1 ms after the power level has been changed.

Three different model assumptions are compared:

(1) χ_e^{pb} remains unchanged,

(2) starting from the steady-state value, χ_e^{pb} is modified proportionally to $T_e^{3/2}$, and

(3) the steady-state value of χ_e^{pb} at the new power level is used.

All steady-state values are taken from power balance analyses in the stationary phases. The experimental results are best reproduced by assumption (3) for the time developments following the switch-on and switch-off phases (see Fig. 2).

Surprisingly, the comparison suggests that 1 ms after the heating power has changed, χ_e^{pb} already has adjusted throughout the profile to the level expected for the steady state of the modified power level. The change is much faster than the modifications of $T_e(r)$ and $\nabla T_e(r)$, which follow on the adjusted diffusive time scale. In agreement with the results of the modulation frequency variation, χ_e^{pb} appears not to be explicitly dependent on the electron temperature or the temperature gradient, but seems determined by processes relating to the heating power, which causes a fast propagating mechanism to act on the transport. This model is able to resolve the apparent contradiction between the stationary and perturbative analyses: while χ_e^{pb} increases with both T_e and ∇T_e, as found in power scans, heat wave analysis excludes these dependencies.

The contradiction is solved if χ_e^{pb} does not depend on the local power flux, but on a process governed by the heating power inside the respective flux surface on which it almost instantaneously reacts. Experiments are going on to find an observable quantity that reacts faster than on the diffusive time scale to the change in heating power, using sufficiently time-resolved H_α,

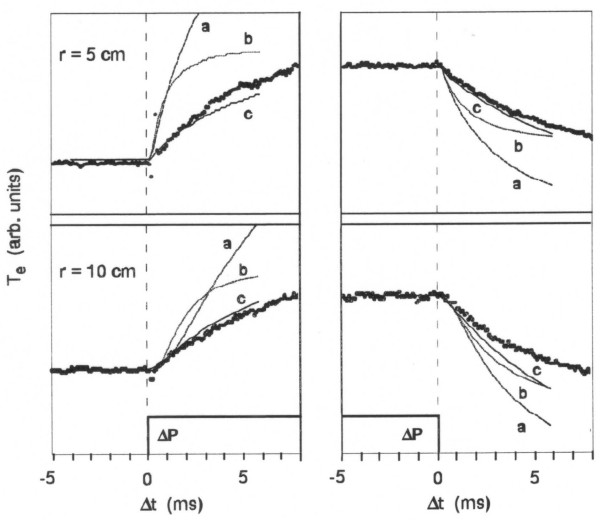

Fig. 2. Time evolution of the electron temperature after switching of the heating power by ΔP. The experimental data are compared with three different simulations: (a): χ_e is unchanged, (b): χ_e is modified proportional to $T_e^{3/2}$, and (c): the steady-state value of χ_e for the new power level is used.

reflectometry, and microwave scattering measurements. Particular attention will be put to changes in the radial electric field as in WVII-A.

References

[1] L. Giannone et al., Nucl. Fusion **32**, 1985 (1992).

[2] H. Hartfuss et al., Nucl. Fusion **26**, 678 (1986).

[3] U. Stroth et al., Local Transport Studies in Fusion Plasmas, 161, Varenna, Italy, 1993.

H. Hartfuss, L. Giannone, U. Stroth,
W7-AS Team, and ECRH Group
IPP Garching, Germany
Phone : 0049-89-3299-1896
E-Mail: hartfuss@wendelstein.ipp-garching.mpg.de

High current negative ion beam obtained for NBI at NIFS

Previously, we reported to have extracted 1.2 A of negative ions with the current density of 54 mA/cm^2 from 36 holes at the center of one-third scale ion source [1]. The extraction area was then increased to 560 holes, and we have now succeeded in extracting 16 A of negative ions with the current density of 45 mA/cm^2, which are the record values [2]. Figure 1 shows accelerated negative ion current as a function of input arc power. The total ion current is measured by a two-dimensional calorimeter array placed 2.3 m downstream from the plasma grid. The accompanied electrons are removed by the magnetic field in front of the calorimeter. A remarkable feature of Fig. 1 is that H^- current increases linearly with the arc power and that it does not saturate yet. The operating gas pressure in this high-current-density experiment was 0.9 Pa. At this gas pressure, the stripping loss of negative ions through the accelerator is estimated at about 30%, which is still a large fraction. The amount of H^- decreased to a half when the ion source was operated at 0.4 Pa.

The operating gas pressure can be reduced if the ionization efficiency is improved, which might be done by increasing the magnetic field strength to confine fast electrons. We have constructed a new one-third scale source for this purpose, where the strength of the magnetic cusp field increases almost twice (from 1 kG on axis to 1.8 kG at the wall), and the magnetic filter configuration is converted from a "rod type" to an "external type" where the filter field is produced by a pair of strong magnets at the side wall of plasma chamber. We

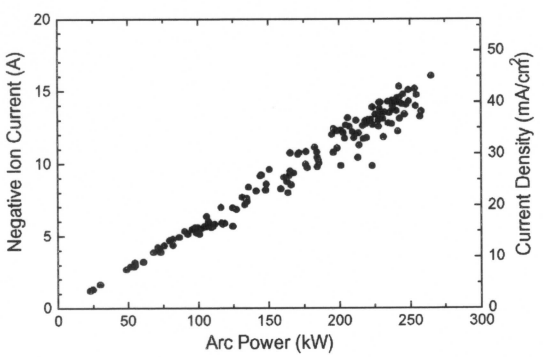

Fig. 1. Dependence of extracted negative ions on the arc power. The right axis shows a corresponding current density. Beam energy is 35 keV.

have obtained 16.2 A of negative ion current at the operating gas pressure of 0.5 Pa) [3], where the corresponding current density is 31 mA/cm^2. 13.6 A of H^- has been accelerated with the energy of 125 keV at 0.4 Pa. Because an external filter can improve transparency of the grid, the arc power efficiency (total ion current / input arc power) can be improved from 0.06 to 0.1 A/kW. The results of our R&D are summarized in Fig. 2 with those of other groups.

Why negative ions?

Neutral injection of 20 MW with a pulse length of 10 s is planned as a main heating method in LHD. Tangential injection is essential here to avoid the loss of deeply trapped fast ions in the helical ripple. The lack of so-called "profile consistency" in helical systems requires that the beam should be deposited at the center of the plasma. These two constraints and the large aspect ratio of the machine (R/a = 6.5) make the required beam energy high (125 keV for hydrogen and 250 keV for deuterium). This energy is higher than that of a conventional neutral beams system (80 keV for hydrogen at most).

For constructing the neutral beam injection system of this energy range, the use of negative ions is inevitable. The neutralizing efficiency is only 13% for the positive hydrogen ion of 125 keV, while remaining 58% for the negative ion of same energy. The negative-ion-based system has some advantages besides its high neutralization efficiency. There are no fractional energy components in the beam. The beam optics are very good, and a bright beam can be obtained, which is very preferable for LHD-NBI because the size of the tangential port is small.

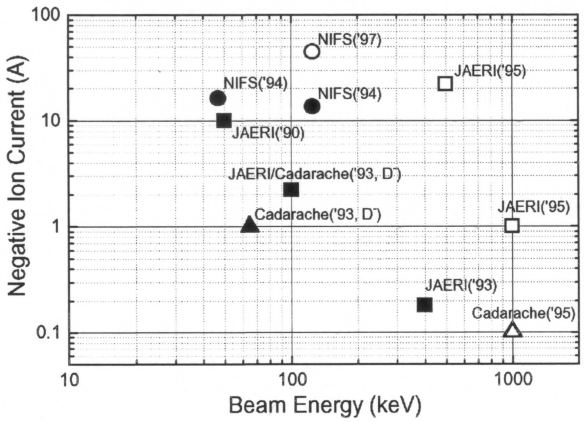

Fig. 2. Summary of the recent development of large current negative ion sources in the world. Closed symbols show the achieved results, and open ones indicate near-future targets.

R&D of a large current negative ion source

The beam energy required for a reactor-relevant large machine such as ITER is higher than 1 MeV, where the development of a high-current accelerator is the key technological issue for a negative-ion-based neutral beam injection system. In the LHD project, however, the required beam energy is low, but we need a large amount of negative ion current: 360 A of negative ion current is needed for 20 MW injection at an energy of 125 keV when the total efficiency is taken to be 45%. At the start of LHD project, the state-of-the-art of high current negative hydrogen ion source was only in the 1-A range. Therefore, the development of a large-current negative ion source is the key technological issue for the LHD project [4], although we can adopt a conventional electrostatic accelerator due to the low beam energy. We are planning our NBI system with four beamlines, each of which has two negative ion sources. We have designed our ion source to deliver 45 A of hydrogen negative ions with a current density of 30 mA/cm^2. We consider that this current density is the minimum necessary to design an ion source of realistic size (the extraction area is 25 cm × 150 cm with a transparency of 40%). These are our R&D target values.

The R&D project was started in 1989. In the research, one-third scale negative ion sources have been studied mainly, which have an extracting area of 25 cm × 50 cm. The first ion source was designed based on the pure hydrogen discharge. Then, introducing a small amount of cesium vapor into the discharge was found to enhance dramatically the production of negative ions. Our recent results reported here were obtained by using these cesiated discharges. We are carrying forward R&D at the test stand that was constructed at Toki in 1992. The test stand was designed based on the conceptual design of LHD-NBI to test the feasibility of components of the NBI system, such as neutralizer, beam dumps, cryopumps, and so on. The power supply system can operate a full-scale ion source. We are now proceeding with a detailed design of the injector. The final design of the neutral beam injector will be finished in 1995, and the construction will start in 1996. The beam injection experiment is scheduled in 1998.

References

[1] T.Kuroda, A.Ando, K.Tsumori, Y.Takeiri, O.Kaneko, Y.Oka, *Stellarator News*, Issue 27 (1994).

[2] A.Ando, K.Tsumori, Y.Oka, O.Kaneko, Y.Takeiri, E.Asano, T.Kawamoto, R.Akiyama and T.Kuroda, to be published in Phys. of Plasmas.

[3] Y.Takeiri, A.Ando, O.Kaneko, Y.Oka, K.Tsumori, E.Asano, R.Akiyama, T.Kawamoto, T.Kuroda,

M.Tanaka and H.Kawakami, submitted to Rev. Sci. Instrum.

[4] A.Iiyoshi, in Proc. of the 13th Symp. on Fusion Engineering, Knoxville, Vol.II, p.1009 (1989).

Osamu Kaneko for the NBI group
Plasma Heating Division
National Institute for Fusion Science
Oroshi, Toki, 509-52 Japan

Phone: 81-572-57-4079 (ext.246)
Fax: 81-572-57-7135
E-Mail: kosamu@nifsbbs.nifs.ac.jp

The ATF finale

The final stage of the ATF experiments, described in part in the last *Stellarator News*, was completed on July 21, 1994. This operation achieved pulse lengths longer than one hour, obtaining experience useful for future toroidal devices (e.g., LHD and TPX). Some dimensionless scaling experiments were also conducted.

In the last report we described a long-pulse discharge whose pulse length exceeded an hour. We made another attempt as the last shot (#21380) of the ATF operation, achieving a pulse length of 4667 s (1 h17 min), which is comparable to that achieved on the Japanese TRIAM-1M tokamak (1 h 11 min).

In these long-pulse operations, a strip chart recorder proved very useful for real-time monitoring and control. Figure 1 reproduces monitor signals of the strip chart recorder during the longest shot. These signals reveal several adjustments made during the long pulse to circumvent several limitations in the ATF long-pulse operation. To keep the vessel wall temperature below 150°C, the ECH power was reduced to about 70 kW shortly after the initiation. The electron density had to be maintained below the cut-off density ($5 \times 10^{18} m^{-3}$) of the second harmonic 28-GHz ECH. We used density feedback control with manual adjustments of the reference value to maintain vessel pressure below 2×10^{-3} Torr l/s.

Because of the low ECH power used, power loss due to atomic processes (ionization, radiation, and charge exchange) was significant, keeping the electron temperature below the apparent burn-out threshold value. However, higher temperature can be obtained by reducing such atomic-process-related losses and/or higher ECH power. Feedback using the vessel pressure (rather than plasma density) tends to reduce neutral density in the plasma, leading to a higher electron temperature. Hydrogen (rather than helium) discharges tend to have higher electron temperatures (up to 200 eV) due to lower ionization losses. However, hydrogen operation longer than 20 min was not possible because of lack of density control due to desorption of hydrogen on the wall.

Long-pulse operation provided very effective wall conditioning. The total input power to the plasma during one ATF long pulse was about 380 MJ (1×0.08 MW $\times$ 4700 s). This power approximately corresponds to one thousand shots with full NBI in ISX-B ($10^4 \times 1.5$ MW $\times 0.25$ s), or one dozen high-power shots on TFTR (12 $\times 30$ MW $\times 1$ s). Indeed, substantial reduction of low-Z

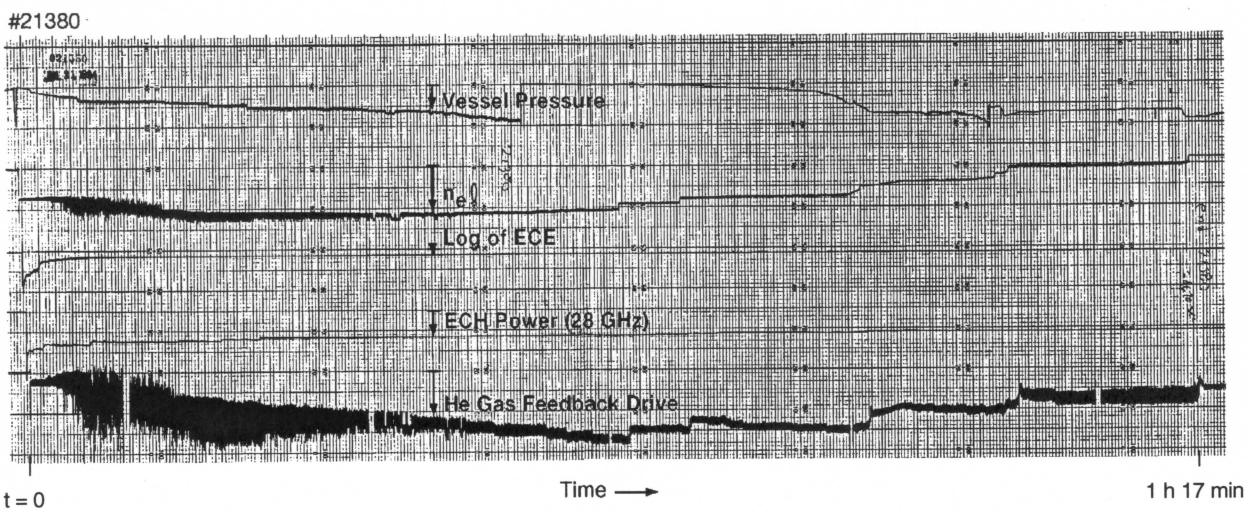

Fig. 1. Strip chart of the longest ATF shot.

impurities was observed during the single long-pulse shot. The residual gas analysis (RGA) data showed that mass-18 (H_2O) level decreased to a record low level, without using any gettering, in a few days after a vent.

Dimensionless parameter scaling experiments took the advantage of the ATF long-pulse capability. In the previous ATF experiments, modulation of dimensionless parameters (ν^* and β) was used to determine an additional dependence to the gyro-Bohm scaling: $\tau_E/\tau_{gB} \propto \nu^{-0.18}\,\beta^{+0.36}$. However, ρ^* (gyro-radius normalized to minor radius) was also modulated in that experiment. Long-pulse operation afforded an additional flexibility of varying the helical field (B), allowing the three variables (B, n, P) to independently control the three dimensionless parameters (ρ^*, ν^*, β^*). By employing two discrete ECH heating frequencies (28 and 35 GHz) and by adjusting their power, the magnetic field, and the plasma density, it was possible to maintain fixed plasma beta and collisionality while varying the normalized gyroradius by 16%, as shown in Fig. 2. A preliminary analysis of the ratio of the energy confinement times at B = 0.65 to 0.50 T ranges between 2 and 1.5. This value is even higher than that expected from gyro-Bohm scaling (1.3), let alone that from Bohm scaling (1.09). These results generally imply the gyro-Bohm-like scaling, which is consistent with the earlier results.

Although limited in many ways (time, resources, plasma parameters, and diagnostics), the final stages of the experiments were very beneficial in gaining experience useful for long-pulse operations on future toroidal devices. The ATF device is now mothballed. However, with minor modifications to add vessel cooling, ATF could be operated as a steady-state technology and/or material test facility.

References

[1] *Stellarator News*, Issue 34 (July 1994).

[2] S. Itoh et al., Plasma Physics and Controlled Nucl. Fus. Res. (Proc. 13th Int. Conf., Washington DC, 1990), **1**, IAEA, Vienna (1991) 733.

Masanori Murakami for the ATF Team
Fusion Energy Division
Oak Ridge National Laboratory
P.O. Box 2009, Oak Ridge, TN 37831-8072

Phone: (615) 574-1175
FAX: (615) 576-7926
E-mail: murakami@fed.ornl.gov

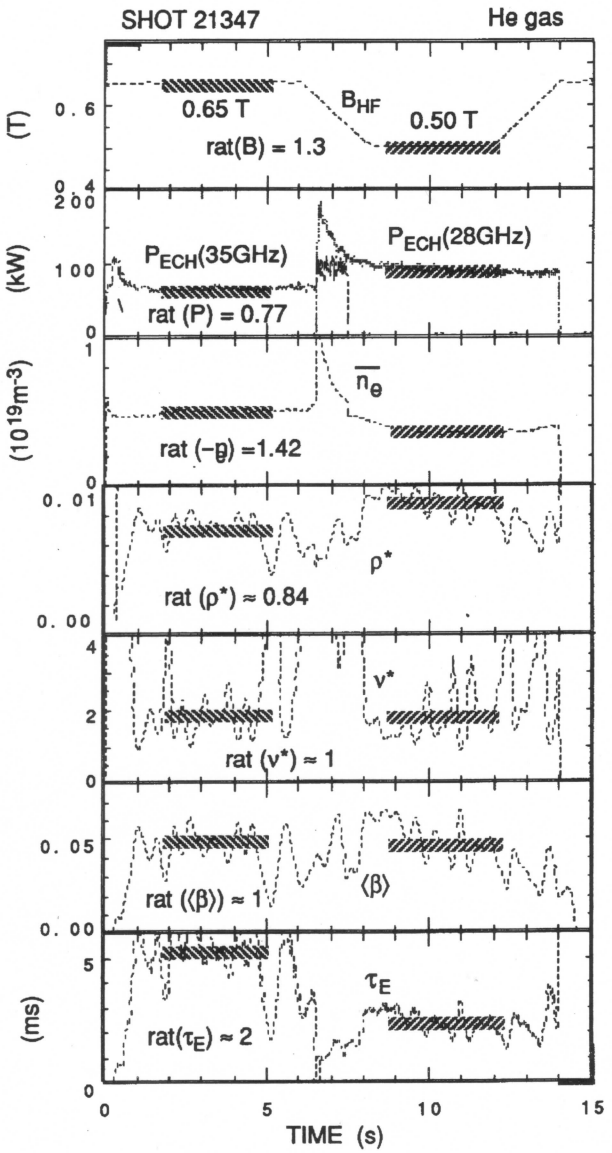

Fig. 2. In this scan, the normalized gyroradius, ρ^*, was varied by 16% while plasma beta and collisionality were held fixed.